



Journal of Advanced Research in Fluid Mechanics and Thermal Sciences

Journal homepage:
https://semarakilmu.com.my/journals/index.php/fluid_mechanics_thermal_sciences/index
ISSN: 2289-7879



CFD Analysis of the Influence of Marine Fouling on the Performance of High-Speed Planning Craft

Ahmad Firdhaus¹, Parlindungan Manik^{1,*}, Muhammad Luqman Hakim¹, Kiryanto¹

¹ Department of Naval Architecture, Faculty of Engineering, Diponegoro University, Semarang, Indonesia

ARTICLE INFO

Article history:

Received 11 July 2023
Received in revised form 29 September 2023
Accepted 12 October 2023
Available online 24 October 2023

Keywords:

Planning hull; marine fouling; CFD; ship performance

ABSTRACT

Marine fouling, such as heavy slime, is the result of algae and other invertebrates settling and growing on the surfaces of planning hulls that are immersed in water. This may result in a range of serious and costly economic problems. The amount of resistance that planning hulls encounter when operating in maritime settings is an important aspect that considerably impacts the performance, energy efficiency, and operational expenses associated with these hulls. Because of this, the focus of this investigation will be on high-speed planning craft ships. In recent years, there has been a rise in the number of instances in which this sort of ship has been used for military, commercial, and recreational purposes. With the use of CFD analysis, the purpose of this study is to conduct an exhaustive investigation into the effect that the surface roughness of heavy slime has on the resistance of planing hulls. The results will be compared to a reference scenario, including a hydrodynamically smooth hull, to determine how much heavy slime affects resistance. According to the findings of this research project, the presence of heavy slime on the surface of a high-speed planing ship had a significant impact on the performance of the ship, particularly on the friction resistance, which saw an increase of up to 65% as a consequence of the presence of the slime. The results of this study will have substantial repercussions for ship designers, naval architects, and operators. The findings will provide them with useful information that will allow them to improve hull designs and devise effective tactics for fouling management.

1. Introduction

The usage of high-speed planing boats for military, commercial, and recreational purposes has risen in recent years [1]. Typical operating speeds have increased due to the development of lightweight engines and propulsion systems. Material and structural research has resulted in the construction of stronger hulls, which are often the limiting factor for the operation of people aboard high-speed planning vessels [2]. Increased fuel consumption, which is dangerous for the environment and unfavorable for business, is a downside of these advancements. Carbon-based fuel is presently the sole viable option for ship propulsion, however alternatives such as wind and solar power are

* Corresponding author.

E-mail address: parlindungan_manik@live.undip.ac.id

<https://doi.org/10.37934/arfmts.110.2.124137>

being developed [3]. As a result, reducing fuel usage is critical for ship industries. As a result, ship industries have endeavoured to discover the optimal hull design, operation and maintenance procedures in order to either reduce operational costs or raise the company's profit [4-11].

Marine fouling, such as heavy slime, is caused by the settling and development of algae and invertebrates on the surfaces of submerged items, and it may cause a variety of significant and expensive economic difficulties [7,12,13]. One of the most well-known impacts of fouling is the reduction in the efficiency with which ships travel. Fouling may significantly enhance the roughness of a ship's underwater sections. This causes a significant increase in frictional resistance to movement through the water, resulting in a significant loss of speed or increased fuel expenditure to maintain the regular operating speed [14]. The resistance experienced by planing hulls during their operation in marine environments is a critical factor that significantly affects their performance, energy efficiency, and operational costs [15,16]. Assessing marine fouling and its impact on planing hull resistance requires a detailed understanding of the complex fluid dynamics involved.

Academic and industrial communities have recently shown a heightened focus on the effect of marine fouling on hull performance in terms of ship resistance and propulsion. The desire to improve fuel economy is driving changes to ship hull design, positively affecting both the bottom line and the environment. The work focuses on four main areas to measure, understand, and predict: hydrodynamic forces in calm water and waves [17-19]. investigation on the roughness effect on ship resistance using Computational Fluid Dynamics (CFD) [20-23]. De Luca *et al.*, [24] presented the findings of a thorough Verification and Validation campaign of resistance test simulations in still water employing Naples Systematic Series warped planing hulls. The research shows simulation uncertainty and comparison errors for various speeds and hull forms. This research used Star-CCM+ for all simulations. Song *et al.*, [25] and Haase *et al.*, [26] demonstrated that the CFD method might be used to accurately anticipate the impact of sand particle roughness on the frictional resistance of flat plates and the resistance of catamarans.

This research intends to completely examine the impact of heavy slime surface roughness on planing hull resistance using CFD analysis. The research will apply state-of-the-art CFD methods to predict the flow around a planing hull with heavy slime surface roughness to do this [21,27]. In the study of ship hydrodynamics, potential and viscous flow models are widely used to simulate and investigate the flow patterns around ships. Potential flow programs using the boundary element approach are utilized to explore free surface wave production [28,29]. Potential flow programs used the Rankine source approach to study ship hull-wave interactions or simulate wave resistance [30]. Viscous flow programs may mimic free surface difficulties like wave-making resistance. These codes use two main methods for free surface computations: the interface-tracking technique (e.g., a moving mesh) and the interface-capturing method (VoF) [31,32]. To simulate planning vessel operations, the numerical simulations will evaluate various velocities, angles of attack, and trim angles. The parametric analysis will explore how heavy slime heaviness affects planing hull resistance. The data will be compared to a hydrodynamically smooth hull reference scenario to determine how much heavy slime increases resistance. The project will also examine heavy slime surface roughness fluid dynamics. The research analyzes flow topologies and pressure distributions to understand how heavy slime influences planing hull resistance. This information will help us understand the physics and devise techniques to limit heavy slime's impact on the planning hull.

The findings of this research will have significant implications for ship designers, naval architects, and operators, providing them with valuable information to optimize hull designs and develop effective fouling control strategies. By quantifying the impact of heavy slime surface roughness on planing hull resistance, this study aims to contribute to enhanced performance, improved energy efficiency, and reduced operational costs in the maritime industry.

2. Methodology

2.1 Free-Surface Flow Solver

This work uses CFD simulations with experimental and numerical data from prior studies to validate the research technique. The Planing Hull Model C seen in Figure 1 is characteristic of fast patrol boats and racing yachts [2]. The transom deadrise angle of this model is 22.5 degrees, and the L/B ratio is 4.3. Table 1 provides the primary dimensions of the specified model C.

Table 1

Principal dimension of the Planing Hull Model C [2]

| Principal Dimension | Full Scale |
|---------------------|------------|
| LPP (m) | 2.0 |
| B (m) | 0.46 |
| T (m) | 0.09 |
| Δ (N) | 243.40 |
| β (°) | 22.5 |
| L/B | 4.35 |

The ISIS-CFD flow solver for EMN (Equipe Modélisation Numérique) uses the RANSE (incompressible unsteady Reynolds-averaged Navier Stokes equations). Using the finite volume method, the solver discretizes transport equations spatially. The face-based method is used to unstructured two-dimensional, three-dimensional, or rotationally symmetric meshes with non-overlapping control volumes constrained by any number of constitutive faces. For incompressible multi-phase viscous fluid flow in isothermal conditions, Eq. (1) to Eq. (3) provide mass, momentum, and volume fraction conservation equations:

$$\frac{\partial}{\partial t} \int_V \rho dV + \int_S \rho (\mathbf{U} - \mathbf{U}_d) \cdot \mathbf{n} dS = 0 \quad (1)$$

$$\frac{\partial}{\partial t} \int_V \rho U_i dV + \int_S \rho U_i (\mathbf{U} - \mathbf{U}_d) \cdot \mathbf{n} dS = \int_S (\tau_{ij} I_j - p I_i) \cdot \mathbf{n} dS + \int_S \rho g_i dV \quad (2)$$

$$\frac{\partial}{\partial t} \int_V c_i dV + \int_S c_i (\mathbf{U} - \mathbf{U}_d) \cdot \mathbf{n} dS = 0 \quad (3)$$

In Eq. (1) to Eq. (3), V is a control volume bordered by a closed surface S moving at \mathbf{U}_d . With a unit normal vector \mathbf{n} pointing outward. \mathbf{U} and ρ are velocity and pressure fields. I_j is a vector whose components disappear except for the j component, which is unity. The viscous stress tensor and gravity vector are I_j and g_i , respectively. c_i is the i -th volume fraction for fluid i and indicates its existence or absence.

The SST (shear-stress transport) model, developed by Menter [33-36], contains several advantageous features from earlier two-equation models. This model mixes model coefficients zonally and restricts eddy viscosity growth in fast strained flows. Zonal modeling makes use of the Wilcox's model close to solid walls and a formulation of the standard model at boundary layer edges and free-shear layers. By limiting turbulent shear stress to a constant multiple of the turbulent kinetic energy inside boundary layers (a realizability restriction), shear stress transport modeling impacts eddy viscosity. With this modification, flow prediction with significant unfavorable pressure gradients and separation is improved. The transport equations for the SST k- ω model are as follows:

$$\frac{\partial}{\partial t}(\rho k) + \frac{\partial}{\partial x_i}(\rho k u_i) = \frac{\partial}{\partial x_j} \left(\Gamma_k \frac{\partial k}{\partial x_j} \right) + G_k - Y_k \quad (4)$$

$$\frac{\partial}{\partial t}(\rho \omega) + \frac{\partial}{\partial x_i}(\rho \omega u_i) = \frac{\partial}{\partial x_j} \left(\Gamma_\omega \frac{\partial \omega}{\partial x_j} \right) + G_\omega - Y_\omega + D_\omega \quad (5)$$

G_k generates turbulent kinetic energy owing to mean velocity gradients in Eq. (4) and Eq. (5), whereas G_ω reflects the production of ω . Turbulence causes k and ω to dissipate, which are represented by Y_k and Y_ω , respectively. In addition, D_ω stands for the cross-diffusion term, whereas Γ_k and Γ_ω denote the effective diffusivity of k and ω , respectively. The beginning and magnitude of flow separation may be accurately predicted using this turbulence model [37].

The influence of wall roughness is considered in the current implementation by employing the equivalent sand particle roughness, H_r . In the turbulence model. Computation is always done on a smooth wall. Dirling's correlation, which ties sand grain roughness to mean roughness height H_r , is used to calculate the equivalent sand grain roughness H_r .

$$H_r = ah \quad a = \begin{cases} 0.0164 \Lambda^{3.780}; \Lambda < 4.93 \\ 139.0 \Lambda^{-1.90}; \Lambda > 4.93 \end{cases} \quad (5)$$

$$\Lambda = \frac{L}{h} \left(\frac{A_S}{A_P} \right)^{4/3} \quad (6)$$

In Eq. (5) and Eq. (6), H_r represents the average roughness height. When there are N roughness elements spread throughout an area S , the average distance between them is denoted by $L = \sqrt{S/N}$. Surface roughness, represented by A_P , is a surface normal to the flow direction that is projected onto a plane. This study represents marine fouling using heavy slime conditions based on Schultz [38] with detailed properties in Table 2 below

Table 2

Value of equivalent sand roughness height (K_s) and coating roughness ($R_{t_{50}}$) of heavy slime [38]

| Description of condition | Heavy slime |
|--------------------------|-------------|
| NSTM rating (NSTM 2002) | 30 |
| K_s (μm) | 300 |
| $R_{t_{50}}$ (μm) | 600 |

2.2 Modeling, Meshing, and Boundary Conditions in Geometry

Figure 1 and Figure 2 depict a 3-D CAD model of the designated model C hull form and mesh of the computational domain incorporating the designated model C. The geometry was generated using the FINETM/Marine modules C-Wizard and HEXPRESS, the NUMECA grid generator [39]. The C-Wizard plugin guides users through mesh and solver parameter configuration. The domain is constructed by designating a frame around the ship, and the length of the ship determines the extent of the computational domain. Due to the ship's symmetry, only half of it was simulated.

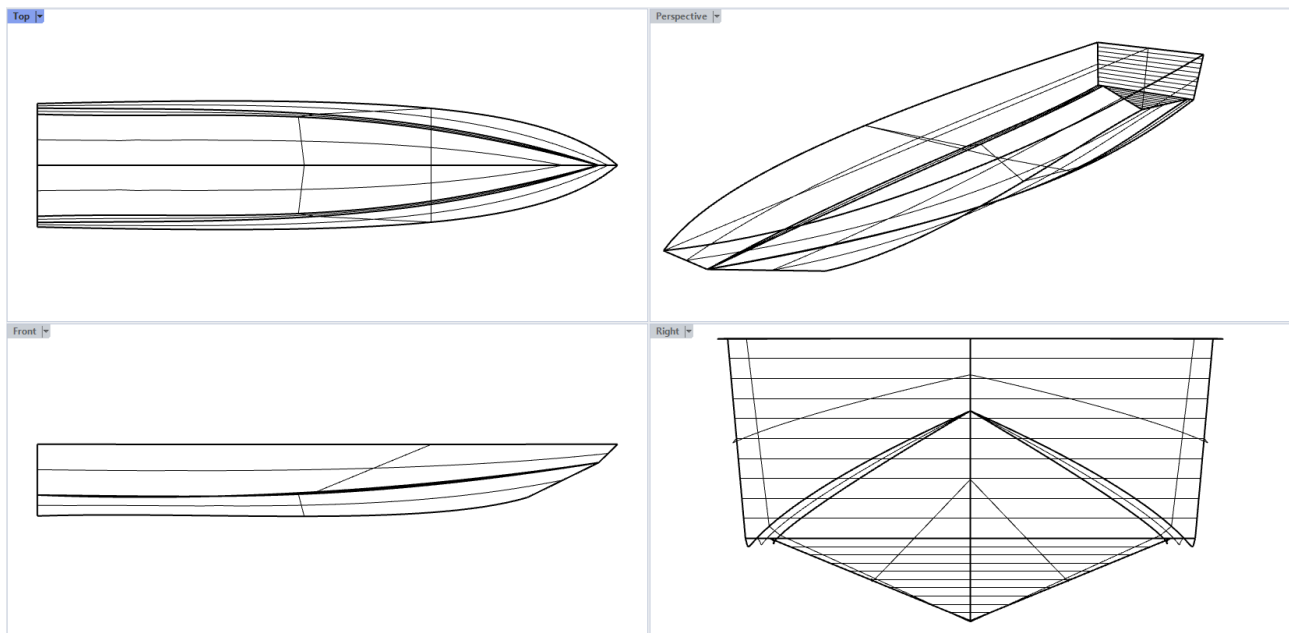


Fig. 1. A 3-D CAD model of the designated model C hull form

As can be seen in Figure 2, the computational domain has the following boundary conditions [40]. The inlet was positioned 1 L upstream of the model. The outlet was positioned 3.0 L aft, near the back of the model. The sidewall was located at a distance of 1.5 L from the waterline. Inlet, outlet, and sidewall boundary conditions were all set to the same free stream far-field velocity. Boundary conditions were established as a prescribed pressure, and the bottom and top walls were situated 1.50 L below and 1.0 L above the model, respectively. A wall function was used as the no-slip boundary condition on the ship's hull. The simulations also fixed the heave and pitch movements. Per-patch roughness with varying roughness values has been applied to each wall-function patch. The heavy slime texture option with sand particle height definition characterizes the hull's surface below the waterline. In contrast, the deck's surface is hydrodynamically smooth, as shown in Figure 2(b).

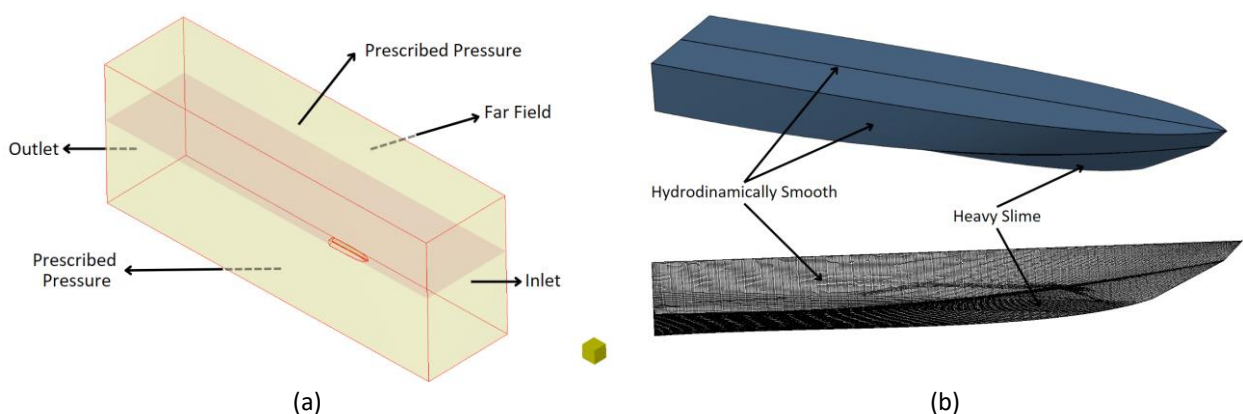


Fig. 2. (a) Computational domain with the simulation model and (b) boundary conditions on the surface of the simulation model

2.3 Grid Independence

Numerical experiments were conducted to ascertain the optimal grid size (number of cells) and to probe the convergence of the numerical solution to meet the grid-independence criteria [41]. In these simulations, the overall ship resistance (R_T) was determined by raising the simulation's cell amount. Two further simulations resulted in a number of cells around 1.5-2 times larger than the original population. The time required to complete each simulation was compared to one another, and the resulting discrepancy was expressed as a percentage inaccuracy.

Table 3 and Figure 3 show a consistently decreasing trend in R_T as a function of simulation cell count, with the trend reaching an asymptotic value as the cell count approaches infinity. With a percent error of 0.02%, 2091569 cells (run number 6) are regarded as the optimal amount of cells, much below the 2% indicated in Hughes [42].

Table 3

Total ship resistance (R_T) is determined by increasing the simulation's cell count

| Simulation | Cells Amount | R_T (N) | Percentage error [%] |
|------------|--------------------|-----------|----------------------|
| 1 | 0.16×10^6 | 35.30 | |
| 2 | 0.28×10^6 | 34.45 | -2.41% |
| 3 | 0.54×10^6 | 33.84 | -1.75% |
| 4 | 1.01×10^6 | 33.60 | -0.73% |
| 5 | 1.55×10^6 | 33.59 | -0.02% |
| 6 | 2.09×10^6 | 33.60 | 0.02% |

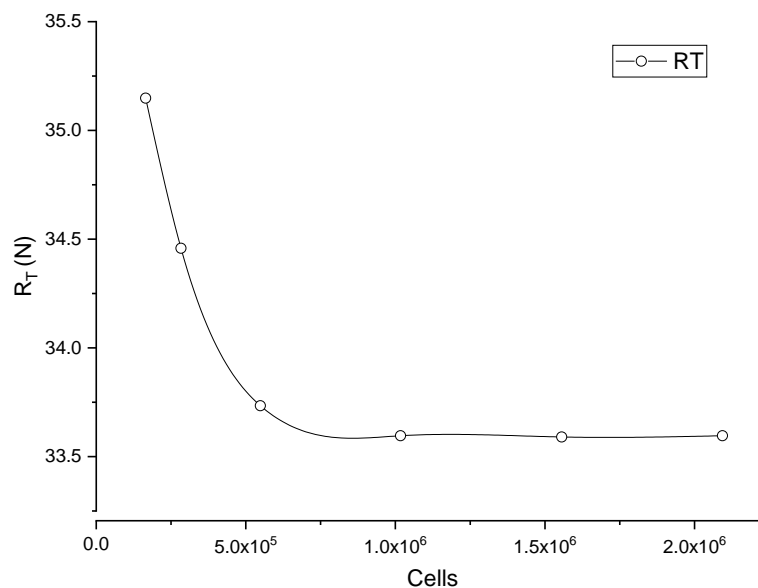


Fig. 3. Total ship resistance R_T as a function number of cells used in the simulation

3. Results

3.1 Validation Study

To begin, the hydrodynamically smooth and heavy slime planning hull model C is fully analyzed at the total speed range to obtain the total resistance coefficient of the ship, where the simulation results in the total resistance of the ship R_T , which can be converted into the coefficient of the total resistance of the ship, or C_T , using a formula based on ITTC [43]. As shown in the formula below, S is

the ship's hydrostatic wetted surface area, ρ is the water density under simulation conditions, and U represents the ship's speed.

$$C_T = \frac{R_T}{\frac{1}{2}\rho S U^2} \tag{5}$$

Table 4 and Figure 4 compare the numerical simulation results to the experimental data from Taunton *et al.*, [2], where only one process validation parameter, total resistance, was examined. Other parameters, including dynamic trim and dynamic sinkage, will be covered in the following section. Comparison of CFD and EFD results reveals that the errors are substantial at both ends of the speed spectrum. The minimum error occurs when errors are significant at both ends of the speed spectrum. The greatest error occurs at midship velocities, whereas the high-speed range has a greater error rate and is inconsistent.

Nevertheless, more research is needed to understand the discrepancies seen at greater speeds. It's possible that the inconsistency in the numerical model between cell size and ship speed causes the mistakes to become more pronounced at greater speeds, as is often the case with numerical simulations. When applied to ship resistance, the following study's criteria show that the resistance prediction is within a respectable level, with an average absolute error value of not more than 5%, which is more than acceptable for resistance simulations.

Table 4

Percentage comparison error between experimental and CFD for ship resistance coefficient

| Fr | Experiment [2] | CFD | Percentage error |
|------|-----------------------|-----------------------|------------------|
| 0.91 | 6.39×10^{-3} | 6.25×10^{-3} | -3.11% |
| 1.41 | 5.43×10^{-3} | 5.24×10^{-3} | -5.68% |
| 1.84 | 4.68×10^{-3} | 4.49×10^{-3} | -7.53% |
| 2.28 | 4.29×10^{-3} | 4.08×10^{-3} | -7.44% |
| 2.72 | 4.27×10^{-3} | 4.00×10^{-3} | -5.43% |

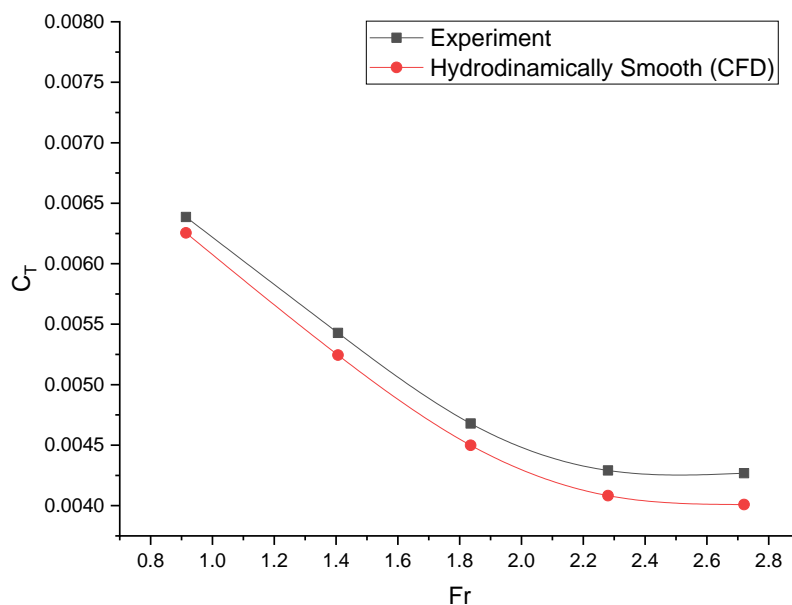


Fig. 4. Coefficient of total ship resistance C_T as a function number of cells used in the simulation

3.2 Pitch and Heave

The induced resistance is proportionate to the pressure created by the hull, which determines how the trim of the vessel is adjusted. The comparison of the trim at different Froude numbers is seen in the Table 5 and Figure 5. The overall trim in the model C planing hull follows the same pattern, although the value obtained from the experiment is higher than predicted by the CFD calculations. The range of trim angles is between 0.965° and 2.807° . The greatest trim angle discovered for CFD on heavy slime surface conditions and Fr 0.91 is 2.420° , whereas the maximum trim angle discovered from experimental data at the same Fr is 2.807° . The application of heavy slime to the surface of the ship leads to an increase in the trim value in comparison to hydrodynamically smooth, particularly at $Fr < 1$ around 14%, and declines with increasing craft speed, except at relatively low speed, which is following the findings of Ghassemi and Ghiasi [44].

Table 5

Comparison of trim values between EFC and CFD of hydrodynamically smooth and heavy slime surface

| Fr | Trim (deg) | | CFD-EFD percentage difference (%) | Hydrodynamically smooth and heavy slime percentage difference (%) | |
|------|------------|-------------------------|-----------------------------------|---|-------|
| | EFD | CFD | | | |
| | | Hydrodynamically Smooth | | | |
| | | Heavy slime | | | |
| 0.91 | 2.807 | 2.120 | 2.420 | -24.47 | 14.15 |
| 1.41 | 2.681 | 2.642 | 2.848 | -1.43 | 7.77 |
| 1.84 | 2.002 | 2.033 | 2.135 | 1.55 | 5.04 |
| 2.28 | 1.746 | 1.384 | 1.437 | -20.72 | 3.83 |
| 2.72 | 1.739 | 0.965 | 0.996 | -44.52 | 3.25 |

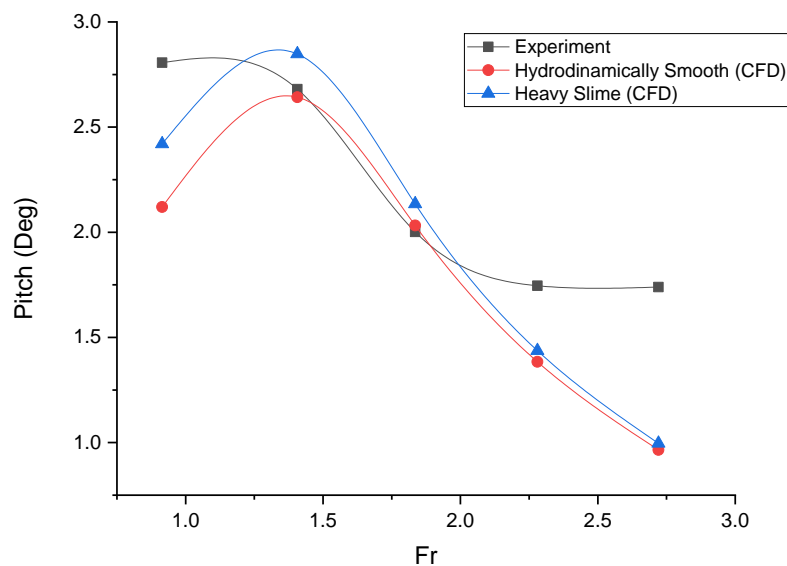


Fig. 5. Pitch (deg) as a function of ship speed (Fr)

The vertical oscillations experienced by a planing ship are referred to as the heave motion. This motion is caused by the ship's ability to skim over the water's surface. The dynamic sinkage, as measured by the heave of the planing hull mode C, is compared in Table 6 and Figure 6 between CFD-EFD, hydrodynamically smooth surfaces, and heavy slime surfaces at five different speeds. There is less than a 5% margin of error between the two sets of findings, yet the dynamic sinkage values from CFD and EFD show the same pattern with rises in speed. For a Fr of 0.91, the surface of heavy slime has a heave value of 0.076 meters, which is 19% more than the smooth surface. However, for Fr

greater than 2, adding heave value is only around 5%. On the surface of heavy slime, there is a tendency toward a situation where the rise in heave value progressively declines with increasing speed. This phenomenon is referred to as the "heave value trend." In the case of a heavy slime surface condition, the presence of irregularities on the hull surface introduces additional hydrodynamic forces. This results in increased vertical accelerations and a less predictable heave motion pattern, which causes the value of heave motion to be greater than it would be with a hydrodynamically smooth surface.

Table 6
 Comparison of heave values between EFD and CFD of hydrodynamically smooth and heavy slime surface

| Fr | Heave (m) | | CFD-EFD percentage difference (%) | Hydrodynamically smooth and heavy slime percentage difference (%) |
|------|-----------|-------------------------|-----------------------------------|---|
| | EFD | CFD | | |
| | | Hydrodynamically Smooth | heavy slime | |
| 0.91 | 0.021 | 0.023 | 0.025 | 17.78 |
| 1.41 | 0.042 | 0.043 | 0.046 | 10.68 |
| 1.84 | 0.051 | 0.052 | 0.054 | 6.69 |
| 2.28 | 0.053 | 0.053 | 0.055 | 4.84 |
| 2.72 | 0.051 | 0.052 | 0.053 | 3.73 |

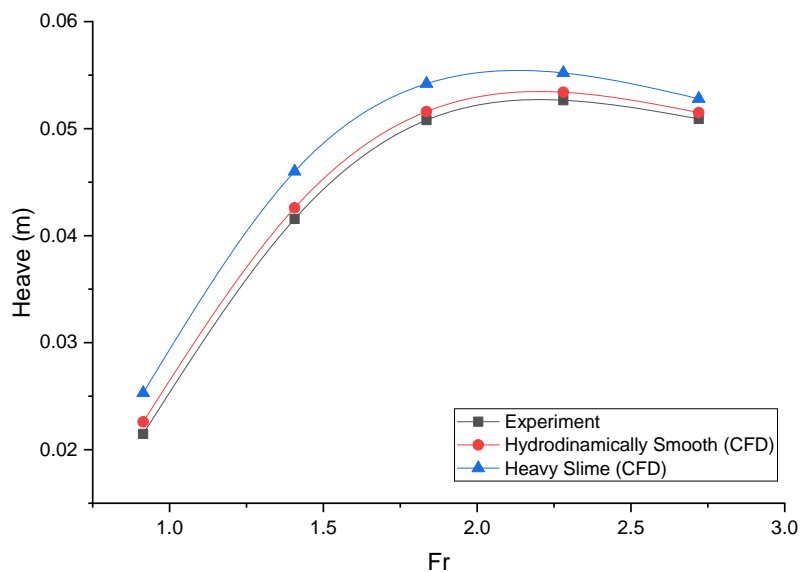


Fig. 6. Heave (m) as a function of ship speed (Fr)

3.3 Frictional Resistance

The frictional resistance of the planing hull type C is illustrated in Table 7 and Figure 7, and it can be derived over a range of 5 different speeds and two separate surface conditions. These tables may be found below. Due to the fact that the values of the frictional resistance obtained via experimentation are not yet available, the table for the frictional drag calculation only includes the results from the CFD simulations.

The findings that were presented in Table 7 and Figure 7 indicated that the increase in R_f of the planing hull model C due to heavy slime at a low ship speed of Fr 0.91 was predicted to be 21.08% and that it gradually increased in line with increasing speed to Fr 2.72, with the largest increase in frictional resistance of 65.65% compared to hydrodynamically smooth surfaces, this is consistent with

findings from studies conducted on Demirel *et al.*, [45], which found that the larger the increase in ship speed, the greater the rise in frictional resistance. Because of this increase in the ship's friction resistance, there would be a large rise in the total ship resistance, increasing the quantity of CO² emission. The conclusions that have been drawn are consistent with the ones that Schultz [38] came to. It is vital to bear in mind that the increase in fuel consumption produced by the roughness of different marine coatings is still a major element when examining the amount of fuel a ship consumes since this is one factor that contributes to the overall amount.

Table 7
 Percentage comparison between CFD frictional resistance of hydrodynamically smooth and heavy slime surface

| Fr | Hydrodynamically Smooth | Heavy Slime | Percentage difference (%) |
|------|-------------------------|-------------|---------------------------|
| 0.91 | 20.468 | 24.782 | 21.08% |
| 1.41 | 38.448 | 51.088 | 32.88% |
| 1.84 | 58.472 | 87.063 | 48.90% |
| 2.28 | 87.246 | 137.537 | 57.64% |
| 2.72 | 121.192 | 200.755 | 65.65% |

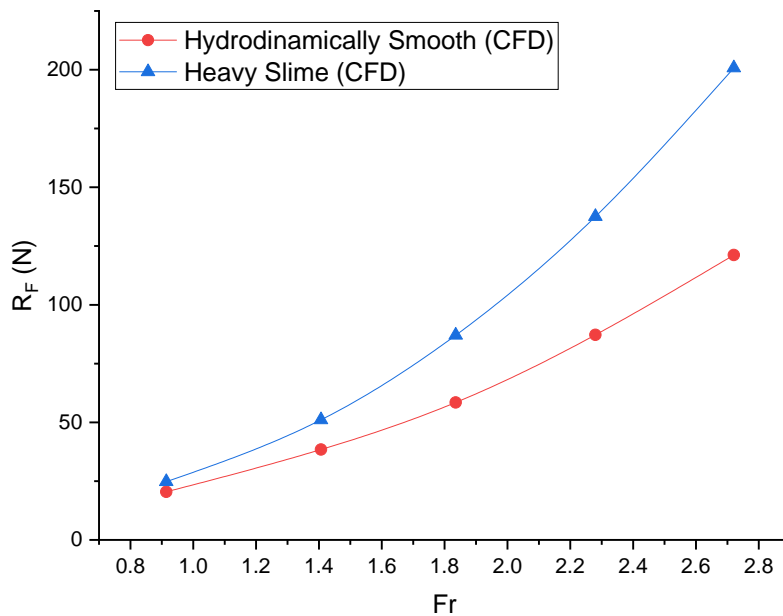


Fig. 7. Frictional Resistance ship R_F as a function of ship speed (Fr)

Viscous stress vectors (fluid to the wall) are shown in Figure 8 from the planing hull model C on two different surface conditions, with the active vector quantity represented as an arrow at a particular mesh node of the hull from the planing hull model C. Figure 8 also includes the active vector quantity. The values for the vector magnitude of viscous stress are represented by the colors ranging from blue to red, with 0 being blue and 60 representing red. Figure 3(a) depicts a lighter green tint around the bow and the complete WSA surface, while Figure 3(b) depicts a blue hue that predominates more of the scene. In addition to the colour, the pattern vectors of viscous stress on heavy slime are more pointed than those on hydrodynamically smooth, which indicates that the frictional forces on the rough surface are more concentrated than those on the smooth surface.

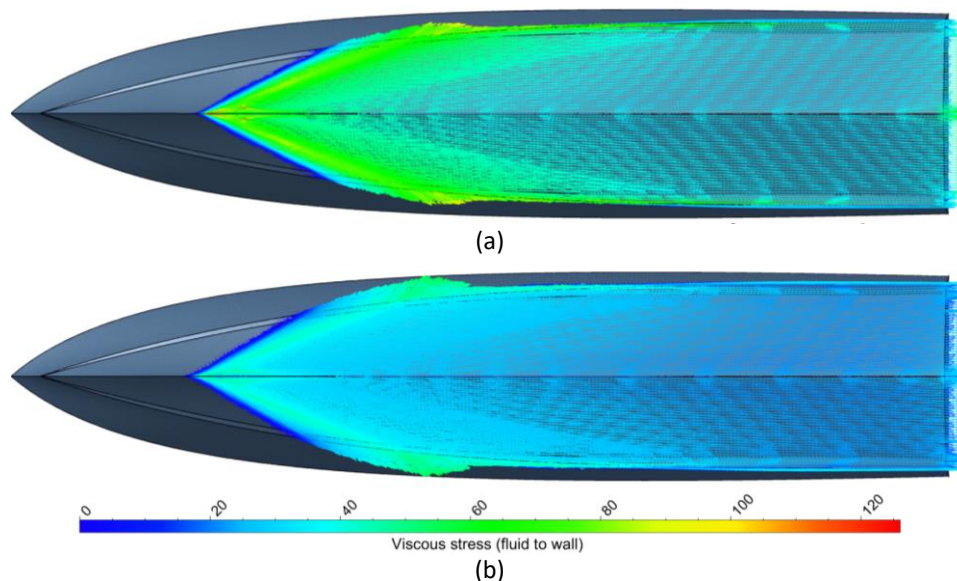


Fig. 8. Visual comparison of viscous stress between heavy slime and hydrodynamically smooth ($Fr=2.72$)

CFD investigation of the planing hull model C showed that the total resistance coefficient prediction is within an acceptable range, with an average absolute error of less than 5% compared to experimental data. The comparison showed errors at low and high speeds, with the biggest mistake at midship speeds. High-speed disparities reflect numerical model errors in cell size and ship speed. Trim research indicated that extensive slime on the hull surface caused larger trim angles than in hydrodynamically clean circumstances, particularly at lower speeds. Except at low speeds, trim value decreased with craft speed. Heave motion, which reflects the planing ship's vertical oscillations, is enhanced with heavy slime on the hull surface, especially at lower speeds. However, the heave value decreased as speed increased, demonstrating a "heave value trend" over the heavy slime surface. The heavy slime surface condition increased hydrodynamic forces, which increased vertical accelerations and made heave motion less predictable, emphasizing the importance of hull surface conditions. The planing hull model C has much higher frictional resistance under heavy slime surface conditions than hydrodynamically smooth surfaces. Heavy slime was anticipated to increase frictional resistance by 21.08% at low ship speeds, rising to 65.65% at $Fr 2.72$. Viscous stress vectors on planing hull model C showed considerable variations between hydrodynamically smooth and heavy slime surface conditions. The heavy slime surface had more pointed vectors, suggesting that frictional forces on the rough surface are more concentrated than on the smooth surface. This concentration of forces increases frictional resistance for the planing ship on heavy muck. Understanding these viscous stress patterns helps optimize hull design and coatings for ship efficiency and decreased resistance.

4. Conclusions

Planing hull model C has been properly simulated numerically using CFD with two distinct hull surface conditions: hydrodynamically smooth and heavy slime. The ship resistance coefficient values were comparable to experimental data to validate the simulation resistance results. Overall, the surface irregularity of a ship's hull with heavy slime affects the ship's performance, particularly in the frictional resistance, where there is a significant increase of up to 65% compared to ships with a hydrodynamically smooth surface, as indicated by n the surface of the heavy slime, the viscous vector patterns were more pointed—indicating that frictional forces are more concentrated on the uneven

surface than on the hydrodynamically smooth surface. This concentration of forces increases the ship's resistance to slipping on heavy sludge. Understanding these viscous stress patterns helps optimize hull design and coatings for increased ship efficiency and decreased resistance.

Acknowledgment

This research was funded by the 2023 Engineering Faculty RKAT Fund, Diponegoro University, with the Strategic Research scheme Number: 44/UN7.F3/HK/V/2023.

References

- [1] Mohamad Ayob, Ahmad F., Ahmad F. Mohamad Ayob, Tapabrata Ray, and Warren Smith. "A hydrodynamic preliminary design optimization framework for high speed planing craft." *Journal of Ship Research* 56, no. 01 (2012): 35-47. <https://doi.org/10.5957/jsr.2012.56.1.35>
- [2] Taunton, D. J., D. A. Hudson, and R. A. Shenoi. "Characteristics of a series of high speed hard chine planing hulls-part 1: performance in calm water." *International Journal of Small Craft Technology* 152 (2010): 55-75.
- [3] Budiyanto, Muhammad Arif, Ardhanu Adha, and Putu Hangga Nan Prayoga. "Distribution of energy efficiency design index for tankers in Indonesia." *Energy Reports* 8 (2022): 170-176. <https://doi.org/10.1016/j.egy.2022.10.089>
- [4] Nazemian, Amin, and Parviz Ghadimi. "CFD-based optimization of a displacement trimaran hull for improving its calm water and wavy condition resistance." *Applied Ocean Research* 113 (2021): 102729. <https://doi.org/10.1016/j.apor.2021.102729>
- [5] Tran, Thai Gia, Quang Van Huynh, and Hyun Cheol Kim. "Optimization strategy for planing hull design." *International Journal of Naval Architecture and Ocean Engineering* 14 (2022): 100471. <https://doi.org/10.1016/j.ijnaoe.2022.100471>
- [6] Utomo, Budi, and Muhammad Iqbal. "Vertical Motion Optimization of Series 60 Hull Forms Using Response Surface Methods." *Kapal: Jurnal Ilmu Pengetahuan dan Teknologi Kelautan* 17, no. 3 (2020): 130-137. <https://doi.org/10.14710/kapal.v17i3.33212>
- [7] Degiuli, Nastia, Andrea Farkas, Ivana Martić, and Carlo Giorgio Grlj. "Optimization of Maintenance Schedule for Containerships Sailing in the Adriatic Sea." *Journal of Marine Science and Engineering* 11, no. 1 (2023): 201. <https://doi.org/10.3390/jmse11010201>
- [8] Hakim, Muhammad Luqman, Bagus Nugroho, I. Ketut Suastika, and I. K. A. P. Utama. "Alternative Empirical Formula for Predicting the Frictional Drag Penalty due to Fouling on the Ship Hull using the Design of Experiments (DOE) Method." *International Journal of Technology* 12, no. 4 (2021): 829-842. <https://doi.org/10.14716/ijtech.v12i4.4692>
- [9] Utama, I. K. A. P., Bagus Nugroho, M. Yusuf, F. A. Prasetyo, M. L. Hakim, I. K. Suastika, Bharathram Ganapathisubramani, N. Hutchins, and Jason P. Monty. "The effect of cleaning and repainting on the ship drag penalty." *Biofouling* 37, no. 4 (2021): 372-386. <https://doi.org/10.1080/08927014.2021.1914599>
- [10] Hakim, Muhammad Luqman, I. K. Suastika, and I. K. A. P. Utama. "A practical empirical formula for the calculation of ship added friction-resistance due to (bio) fouling." *Ocean Engineering* 271 (2023): 113744. <https://doi.org/10.1016/j.oceaneng.2023.113744>
- [11] Abdullah, Jamaluddin, and Halim Mad Lazim. "Malaysia Shipbuilding Industry: A Review on Sustainability and Technology Success Factors." *Journal of Advanced Research in Applied Sciences and Engineering Technology* 28, no. 3 (2022): 154-164. <https://doi.org/10.37934/araset.28.3.154164>
- [12] Schultz, Michael P., J. A. Bendick, E. R. Holm, and W. M. Hertel. "Economic impact of biofouling on a naval surface ship." *Biofouling* 27, no. 1 (2011): 87-98. <https://doi.org/10.1080/08927014.2010.542809>
- [13] Hakim, M. L., B. Nugroho, M. N. Nurrohman, I. K. Suastika, and I. K. A. P. Utama. "Investigation of fuel consumption on an operating ship due to biofouling growth and quality of anti-fouling coating." In *IOP Conference Series: Earth and Environmental Science*, vol. 339, no. 1, p. 012037. IOP Publishing, 2019. <https://doi.org/10.1088/1755-1315/339/1/012037>
- [14] Hakim, M. L., I. K. A. P. Utama, B. Nugroho, A. K. Yusim, M. S. Baithal, and I. K. Suastika. "Review of correlation between marine fouling and fuel consumption on a ship." In *Proceeding of SENTA: 17th Conference on Marine Technology*, pp. 122-129. 2017.
- [15] Savitsky, Daniel, and Michael Morabito. "Surface wave contours associated with the forebody wake of stepped planing hulls." *Marine Technology and SNAME News* 47, no. 01 (2010): 1-16. <https://doi.org/10.5957/mtsn.2010.47.1.1>

- [16] Zou, Jin, Shijie Lu, Yi Jiang, Hanbing Sun, and Zhuangzhuang Li. "Experimental and numerical research on the influence of stern flap mounting angle on double-stepped planing hull hydrodynamic performance." *Journal of Marine Science and Engineering* 7, no. 10 (2019): 346. <https://doi.org/10.3390/jmse7100346>
- [17] Firdhaus, Ahmad, I. Ketut Suastika, Kiryanto Kiryanto, and Samuel Samuel. "Benchmark study of FINETM/Marine CFD code for the calculation of ship resistance." *Kapal: Jurnal Ilmu Pengetahuan dan Teknologi Kelautan* 18, no. 2 (2021): 111-118. <https://doi.org/10.14710/kapal.v18i2.39727>
- [18] Firdhaus, Ahmad, and I. Ketut Suastika. "Experimental and Numerical Study of Effects of the Application of Hydrofoil on Catamaran Ship Resistance." *Revolution* 4 (2022): 104-110.
- [19] Bahatmaka, Aldias, Muhammad Yusuf Wibowo, Andi Abdullah Ghyfery, Muhammad Harits, Samsudin Anis, Deni Fajar Fitriyana, Rizqi Fitri Naryanto et al. "Numerical Approach of Fishing Vessel Hull Form to Measure Resistance Profile and Wave Pattern of Mono-Hull Design." *Journal of Advanced Research in Fluid Mechanics and Thermal Sciences* 104, no. 1 (2023): 1-11. <https://doi.org/10.37934/arfmts.104.1.111>
- [20] Hakim, Muhammad Luqman, Bagus Nugroho, Rey Cheng Chin, Teguh Putranto, I. Ketut Suastika, and I. Ketut Aria Pria Utama. "Drag penalty causing from the roughness of recently cleaned and painted ship hull using RANS CFD." *CFD Letters* 12, no. 3 (2020): 78-88. <https://doi.org/10.37934/cfdl.12.3.7888>
- [21] Suastika, I. K., M. L. Hakim, B. Nugroho, A. Nasirudin, I. K. A. P. Utama, J. P. Monty, and Bharathram Ganapathisubramani. "Characteristics of drag due to streamwise inhomogeneous roughness." *Ocean Engineering* 223 (2021): 108632. <https://doi.org/10.1016/j.oceaneng.2021.108632>
- [22] Hakim, Muhammad Luqman, Niko Maqbulyani, Bagus Nugroho, I. Ketut Suastika, and I. Ketut Aria Pria Utama. "Wind-tunnel experiments and CFD simulations to study the increase in ship resistance components due to roughness." *Journal of Sustainability Science and Management* 16, no. 3 (2021): 144-163. <https://doi.org/10.46754/jssm.2021.04.012>
- [23] Marino, Alessandro, Mehmet Atlar, and Yigit K. Demirel. "An investigation of the effect of biomimetic tubercles on a flat plate." In *International Conference on Offshore Mechanics and Arctic Engineering*, vol. 58844, p. V07AT06A063. American Society of Mechanical Engineers, 2019. <https://doi.org/10.1115/OMAE2019-96276>
- [24] De Luca, Fabio, Simone Mancini, Salvatore Miranda, and Claudio Pensa. "An extended verification and validation study of CFD simulations for planing hulls." *Journal of Ship Research* 60, no. 02 (2016): 101-118. <https://doi.org/10.5957/jsr.2016.60.2.101>
- [25] Song, Soonseok, Saishuai Dai, Yigit Kemal Demirel, Mehmet Atlar, Sandy Day, and Osman Turan. "Experimental and theoretical study of the effect of hull roughness on ship resistance." *Journal of Ship Research* 65, no. 1 (2021): 62-71. <https://doi.org/10.5957/JOSR.07190040>
- [26] Haase, Max, Konrad Zurcher, Gary Davidson, Jonathan R. Binns, Giles Thomas, and Neil Bose. "Novel CFD-based full-scale resistance prediction for large medium-speed catamarans." *Ocean Engineering* 111 (2016): 198-208. <https://doi.org/10.1016/j.oceaneng.2015.10.018>
- [27] Bradshaw, P. "A note on "critical roughness height" and "transitional roughness"." *Physics of Fluids* 12, no. 6 (2000): 1611-1614. <https://doi.org/10.1063/1.870410>
- [28] Hess, John L., and Apollo Milton Olin Smith. "Calculation of nonlifting potential flow about arbitrary three-dimensional bodies." *Journal of Ship Research* 8, no. 04 (1964): 22-44. <https://doi.org/10.5957/jsr.1964.8.4.22>
- [29] Insel, M., and A. F. Molland. "An investigation into the resistance components of high speed displacement catamarans." *Transactions of The Royal Institution of Naval Architects, RINA* 134 (1992).
- [30] Jensen, G., H. Soding, and Z. Mi. "Rankine source methods for numerical solutions of the steady wave resistance problem." In *Symposium on Naval Hydrodynamics, 16th*. 1986.
- [31] Li, Tingqiu, and Jerzy Matusiak. "Simulation of modern surface ships with a wetted transom in a viscous flow." In *ISOPE International Ocean and Polar Engineering Conference*, 2001.
- [32] Raessi, Mehdi, Javad Mostaghimi, and Markus Bussmann. "A volume-of-fluid interfacial flow solver with advected normals." *Computers & Fluids* 39, no. 8 (2010): 1401-1410. <https://doi.org/10.1016/j.compfluid.2010.04.010>
- [33] Menter, Florian R. "Influence of freestream values on k-omega turbulence model predictions." *AIAA Journal* 30, no. 6 (1992): 1657-1659. <https://doi.org/10.2514/3.11115>
- [34] Menter, Florian R. "Performance of popular turbulence model for attached and separated adverse pressure gradient flows." *AIAA Journal* 30, no. 8 (1992): 2066-2072. <https://doi.org/10.2514/3.11180>
- [35] Menter, Florian R. "Zonal two equation kw turbulence models for aerodynamic flows." In *23rd Fluid Dynamics, Plasmadynamics, and Lasers Conference*, p. 2906. 1993. <https://doi.org/10.2514/6.1993-2906>
- [36] Menter, Florian R. "Two-equation eddy-viscosity turbulence models for engineering applications." *AIAA Journal* 32, no. 8 (1994): 1598-1605. <https://doi.org/10.2514/3.12149>
- [37] Bardina, J., P. Huang, T. Coakley, J. Bardina, P. Huang, and T. Coakley. "Turbulence modeling validation." In *28th Fluid Dynamics Conference*, p. 2121. 1997. <https://doi.org/10.2514/6.1997-2121>

- [38] Schultz, Michael P. "Effects of coating roughness and biofouling on ship resistance and powering." *Biofouling* 23, no. 5 (2007): 331-341. <https://doi.org/10.1080/08927010701461974>
- [39] NUMECA International. "FINE/Marine 7.2 Theory Guide." *NUMECA Online Documentation Platform*, 2018.
- [40] Versteeg, H. K., and W. Malalasekera. *An introduction to computational fluid dynamics*. Pearson Education Limited, 2007.
- [41] John, D., and J. R. Anderson. "Computational fluid dynamics: the basics with applications." *Mechanical Engineering Series* (1995): 261-262.
- [42] Hughes, G. *An analysis of ship model resistance into viscous and wave components*. NPL, 1965.
- [43] ITTC. "Recommended Procedures and Guidelines Practical Guidelines for Ship Resistance CFD." *ITTC*, 2014.
- [44] Ghassemi, Hassan, and Mahmoud Ghiasi. "A combined method for the hydrodynamic characteristics of planing crafts." *Ocean Engineering* 35, no. 3-4 (2008): 310-322. <https://doi.org/10.1016/j.oceaneng.2007.10.010>
- [45] Demirel, Yigit Kemal, Osman Turan, and Atilla Incecik. "Predicting the effect of biofouling on ship resistance using CFD." *Applied Ocean Research* 62 (2017): 100-118. <https://doi.org/10.1016/j.apor.2016.12.003>